# MODELLING AXIAL COMPRESSION FATIGUE IN FIBRE ROPES

J W S Hearle, R E Hobbs, M S Overington, and S J Banfield

Tension Technology International Ltd, Lloyds Wharf, 2 Mill Street, London SE1 2BD

## ABSTRACT

The modelling of long-term fatigue performance of twisted ropes has been extended to cover axial compression fatigue. This mode of failure has been observed in use and testing of ropes. It is characterised by sharp cooperative kinking of yarns, which leads to flex fatigue breakage of fibres. A model of pipeline buckling was modified to allow for plasticity in bending. The axial and lateral restraints, which influence the buckling, were derived from the existing rope mechanics model. Axial compression was introduced into the total computational model, in order to predict the form of buckling and the consequent fibre failure. An alternative use of the program is simply to detect conditions in which axial compression occurs as an indication of the occurrence of fatigue.

KEYWORDS :

Ropes, Fatigue, Modelling, Compression, Buckling

## INTRODUCTION

At ISOPE-93, we presented papers on modelling tension and torque properties of ropes and splices [Leech, Hearle, Overington and Banfield, 1993] and on the development of the program to cover long-term fatigue performance [Hearle, Parsey, Overington and Banfield, 1993]. The second paper treated three important fatigue mechanisms, creep, hysteresis heating and internal abrasion, and indicated that the work was being extended to include axial compression fatigue. This extension has now been completed and is the subject of the present paper.

The first reported engineering failure in an aramid rope due to axial compression fatigue was in the mooring lines for the construction ship Ocean Builder I used in the erection of the Lena tower in the Gulf of Mexico in mid 1983 [Riewald, 1986; Riewald, Walden, Whitehill and Koralek, 1986]. The lines were deployed on buoys in 1045 feet of water 4 - 6 weeks before the arrival of the ship. On recovering and tensioning, four ropes failed, reportedly at 20% of rated strength. The failure was very thoroughly investigated and explained in the following way. Torque generated in the ropes led to rotation, causing shear and compressive strains, which in turn led to fibre kinking with an accompanying loss of strength. Laboratory studies and ocean deployments, resulting from the investigation of this failure, gave more examples of kinking occurring due to axial compression. Gross kinks were seen in yarns and severe fibre damage was shown up as strongly dyed bands at regular intervals along the yarns.

More recently, unpublished joint industry studies have shown the occurrence of axial compression fatigue in various types of fibre ropes.

Kinking due to axial compression is a phenomenon that occurs on many scales from mountain ranges to oriented polymer molecules. In fibres, the effects are shown by the presence of kinkbands, which run across the fibres at about 45°, when fibres are uniformly compressed, or, more commonly, on the inside of bends. Repeated flexing of fibres leads to failure, either due to breakdown along kinkbands or to axial splitting from the accompanying shear stresses [Hearle, Lomas, Cooke and Duerden, 1989]. In typical test conditions, failure may occur in around 1000 cycles in aramid fibres [Hearle and Wong, 1977], but polyester and nylon fibres would last longer [Hearle and Miraftab, 1991].

## AXIAL COMPRESSION IN ROPES

If a rope as a whole is subject to an axial compressive force, it will buckle into a smooth curve with a radius that is too large to cause fibre damage. The only exceptions would be for very short lengths of rope or where a rope is restrained from buckling by lateral pressure. The common damaging situation is when a component within a rope is forced into compression, subject to the restraint of neighbouring components. This would not occur in perfect ropes under pure tension; but it can occur in practice under low tension for two main reasons.

The first cause is rope nonuniformity, resulting from effects in manufacturing or subsequent handling and use. If one or more components are longer at zero tension than other components, then the equilibrium state of the entire rope at zero tension will have the longer components in compression and the shorter ones in tension. A critical positive tension is needed to eliminate axial compression in the longer elements. If tension-tension cycling goes down to a lower tension than the critical value, some components will suffer compression-tension cycling with consequent damage to fibres.

The second cause is rope twisting. For example, if a parallel assembly of fibres is twisted in either direction at constant length, the outer layers are forced into longer paths and so develop tension. If the overall rope tension falls below the value developed in this way, the central fibres will be forced into compression. In a simple twisted structure, an increase of twist will cause the central straight components to go into compression, whereas a decrease of twist will compress the outer components. In more complicated rope structures, with twist at several levels, the precise effects will depend on the geometry, but twisting will always force some components into axial compression in the absence of sufficient overall rope tension.

Twisting in tension-tension cycling can develop for two reasons. If the rope is not torque-balanced, tension will cause a torque to develop, and this can lead to the rope twisting against a soft termination, such as a splice. Alternatively, if there is nonuniformity along the rope, different sections of rope will twist against each other. Both effects have been found in practice.

OBSERVATIONS OF AXIAL COMPRESSION

Although the test details remain confidential, samples of ropes, which had been subject to tension-tension cycling in the joint industry study, FIBRE TETHERS 2000, were made available for microscopic examination in the Department of Textiles at UMIST [Hearle and Noone, to be published].

The observed effects, which are illustrated in Fig. 1, included the following:

- a wavy buckling of yarns or strands, at fairly low curvature, which would not be likely to cause serious damage to fibres

- kinkbands running across fibres indicating regions of uniform axial compression

- sharp kinks of fibres as a whole, usually occurring cooperatively across yarns

- breaks of fibres along kinkbands within fibres
- axial splits, which would have been caused by fibre bending

Commonly, the sharp fibre kinks, with internal damage that could be picked out by dyeing aramid yarns, occurred in groups in zig-zag sections separated by straight lengths. This, in turn, led to broken pieces, which were a few millimeters in length, followed by unbroken portions, which were a few centimeters long.

## A THEORETICAL MODEL

The original rope model, as described in the earlier papers, was developed for situations in which components were always under tension. In order to model behaviour at low tensions, provision had to be made for some components to be in compression. In addition, since some frictional force remains when the normal forces generated by the model are zero, the friction equation was changed to $F = a + bN$.

The more serious problem was to incorporate the response to axial compressive force on components in a rope. One possibility is that the fibres yield in uniform axial compression. Values of compressive yield stress are known for many fibres. For example in aramids, the value is about 0.35 Gpa, which compares with a tensile strength of about 4 Gpa.

However, it is likely that components will buckle before the fibres yield. The buckling behaviour depends on the bending stiffness of the components and on the lateral and axial restraint. The theory derives from the Euler condition for the buckling of a free elastic beam, which has led on to treatments of more complicated conditions. The important case to consider is the buckling of yarns within the rope, though the same principles apply to other components.

The most relevant earlier work is by Hobbs on the buckling of heated pipelines [Hobbs, 1984; Hobbs and Liang, 1989]. The comparison with the present problem is shown in Table 1.

| | PIPELINE | FIBRES IN ROPE |
|---|---|---|
| BEAM BENDING | elastic | plastic |
| AXIAL RESTRAINT | friction; N due to self-weight | friction; N due to radial pressure |
| LATERAL RESTRAINT | friction; N due to self-weight | radial pressure |

TABLE 1 : Comparitive actions on pipelines and fibre ropes

The principal advance needed is to extend the Hobbs analysis to cover the plastic bending response. In mathematical form, the restraints are the same in both cases, though the parameters have different meanings. In the pipe-line analysis, both restraints are due to friction under the same constant normal load N, and the quantities involved are the axial friction coefficient and the ratio of lateral to axial friction. Although the lateral restraint is not plastic in a materials science sense, it is in the mechanical sense of being a constant force.

For ropes, the axial restraint is also due to friction, but the normal load is due to the effect of applied tension in generating lateral pressure in a twisted structure plus any contribution from the jacket. The lateral restraint is a direct consequence of the lateral pressure. The values of these restraint forces are computed by the existing model. In contrast to the pipe-line analysis, the restraint forces are not constant in all circumstances: they will increase with applied tension. However, provided the lateral displacement involved in kinking is not large, they are effectively constant as buckles form. This is the justification for the plastic approximation.

In addition to the points mentioned above, the geometry differs from the pipeline case. The axial restraint comes from lateral pressure exerted all round the yarn. The axial resistance to slip per unit length will be given by $2\pi\mu Rp$, where R is yarn radius and p is lateral pressure. The lateral restraint per unit length will be $2Rp$. The beam properties are given by two yarn properties: the initial elastic bending stiffness and the bending moment at which plastic deformation starts.

The elastic analysis for pipelines shows that a number of modes are theoretically possible, as illustrated in Fig. 2. One possibility is continuous overall buckling with a regular wavelength: this is referred to as mode infinity. Alternatively, localised buckles can form at intervals along the line. The preferred form is the lowest energy solution, in combination with the effects of any localised initial out-of-straightness in the pipeline.

For yarns in rope, the Hobbs elastic solution can be used to fix the basic form of buckling. When the critical condition for the onset of plastic deformation is reached, the smooth buckles collapse into sharp kinks to give the forms illustrated in Fig. 3. The plastic solution peels off the elastic solution and determines the subsequent behaviour. Observation has shown that individual filaments kink cooperatively in register with one another in yarns. The model confirms this, by predicting kinks of the right size and spacing. The consequences of cooperative kinking are that:

- filament bending properties should be used

- filament radius should be combined with lateral pressure on the yarn to give lateral restraint, since all filaments are contributing to the lateral displacement

- yarn radius should be used for axial slip since all the filaments are moving together and are not slipping axially relative to one another; strictly there will be some shear involved in kink formation, but this contribution to the deformation energy has been neglected

This is the basis for the main computation, which provides the principal cause of serious damage. The analysis predicts the effective axial yield stress and the kink dimensions.

The analysis can be used with values appropriate to yarn or strand buckling in order to indicate whether it is likely that these modes would be likely to occur in preference to cooperative kinking in yarns. The predicted scale of yarn buckling is much larger than in the observed kink formations. However, it may correspond to the wavy buckling found in some tested ropes. Although the predicted onset of wavy buckling may be correct, plastic lateral restraint would not apply to the continued buckling. The lateral displacements tend to be so large that they would generate considerable additional increase in lateral resistance.

The final stage of the analysis was to integrate the buckling model with the existing model, which provides values of the axial contraction and lateral pressures needed to determine buckling in the compression model. It is necessary to iterate, in order to feed back into the basic model values of the compressive yield stress needed to compute the rope response.

Finally, it is necessary to introduce the effect of kinking in causing fibre breakage. The procedure to be adopted is the same as that for handling abrasion in the existing fatigue model. A "rate-of-damage" parameter, which specifies the number of cycles of kinking needed to cause fibre rupture, has to be specified. The reciprocal of this quantity gives the amount of material lost in one cycle. As before, the computation is carried out sequentially on typical cycles, which are then assumed to be representative of a large number of following cycles before the computation is repeated.

The rate of fibre rupture will depend on the severity of the kinking. This will increase with the amplitude of the kinks, which is given by the analysis, and other local stress conditions. As with the abrasion parameter, this is not a fibre property that is available or easily determined, although guidance can be obtained from the results of tests on flexural fatigue of yarns.

COMPUTATION

The development of the model was programmed as before in Turbo-Pascal, and was validated against pipeline buckling data. To the user, the only obvious change is the addition of an axial compression mode and options throughout to specify structure compactions as well as extensions. The additional parameters, which must be specified, are listed in Table 2, together with values appropriate to a 7-strand aramid rope.

| AXIAL COMPRESSION | Parameter Description | Units | Value for a 7-strand aramid rope |
|---|---|---|---|
| Components at all levels in rope structure | Kinking Life | Cycles | 1000 |
| | Modes to be considered | $\infty$, 1..4 | $\infty$ |
| Components at lowest level(s) in rope structure | Fibre diameter | m | 0.000012 |
| | Fibre linear density | dtex | 1.57 |
| | Fibre yield stress | $N/m^2$ | 500 |

Table 2 : Additional parameters specific to axial compression

Fig. 4 shows a plot of buckling amplitude against axial load in this rope as the axial compressive load on the yarns is increased and the plastic solution peels off the elastic solution. This plot is for the infinite mode, but numerical values do not differ greatly for other modes. The parameter $\Omega$ is the measure of resistance to axial movement and it is worth noting that the value of 5000N/m for this fibre rope is more than 13 times the corresponding value of 380N/m for a steel pipeline in contact with the seabed.

Fig. 5 is a plot of retained strength for the rope cycled at 6 second period, with 1 turn/meter of twist, between 4% and 7% of break load. The computation incorporates all the fatigue modes, creep rupture, hysteresis heating, abrasion and axial compression. Over the first few cycles minuscule hysteresis heating causes a barely perceptible drop in strength. Between $10^3$ and $10^4$ cycles the core yarn of the core strand fails due to axial compression fatigue and assuming this component is no longer able to carry any load produces approximately 3% strength loss. Predominantly due to abrasion, but with contributions from creep-rupture, strength falls rapidly above $10^8$ cycles and break is predicted when the rope strength falls to the peak applied load.

## AN ALTERNATIVE PROCEDURE

The full model enables axial compression to be investigated in detail. However, for many purposes, a simpler procedure is useful. This recognises that what is most important is to know when components go into compression. If this happens, fibre failure is likely in a few thousand cycles in aramids and within a million cycles in polyester. Design and use conditions should therefore be controlled to avoid this situation.

The quasi-static model can be used to predict the boundary between tension and compression for any component at any twist level and with any positive or negative excess length relative to the rope length. Fig. 6(a) shows the tension-compression boundary in the core yarn of the core strand of a perfect rope at different twist levels, Fig. 6(b) shows the boundaries for yarns at the various levels within a rope structure, and Fig. 6(c) shows the effect of excess length in another rope.

## CONCLUSION

The current program is a comprehensive integrated package, which covers the quasi-static tension-torque-length-twist responses of twisted and parallel rope structures and the long-term life as determined by important fatigue effects. In order to become more effective in addressing the variety of specific needs that occur, it is currently being developed as a set of separate programs under the general title OP*TTI*-ROPE. These can be run to make predictions needed to meet the particular engineering needs of ropemakers or rope-users.

## ACKNOWLEDGMENT

The financial support of the US Navy, through NFESC contract N.47408-93-R-7017, in carrying out this analysis and including it in the computer program GEN-ROPE, and the advice and encouragement of Dr Francis Liu are gratefully acknowledged.

## REFERENCES

Hearle, J.W.S., Lomas, B., Cooke, W.D. and Duerden, I.J. (1989). "Fibre Failure and Wear of Materials: an Atlas of Fracture, Fatigue and Durability", Ellis Horwood.

Hearle, J.W.S., and Miraftab, M. (1991). "The Flex Fatigue of Polyamide and Polyester Fibres. Part 1: The Influence of Temperature and Humidity", J. Materials Sci., **26**, 2861-2867.

Hearle, J.W.S., and Noone, P. (to be published). "Observations of axial compression fatigue in fibre ropes".

Hearle, J.W.S., Parsey, M.R., Overington, M.S. and Banfield, S.J. (1993). "Modelling the Long-Term Fatigue Performance of Fibre Ropes", Proc. Third Int. ISOPE Conf., 377 - 383, 1993.

Hearle, J.W.S., and Wong, B.S. (1977). "Flexural Fatigue and Surface Abrasion of Kevlar-29 and Other High-modulus Fibres", J. Materials Sci., **12**, 2447-2455.

Hobbs, R.E. (1984). "In-service Buckling of Heated Pipelines", ASCE, J. Transportation Engineering, **110**, 175.

Hobbs, R.E., and Liang, F. (1989). "Thermal Buckling of Pipelines Close to Restraints", 8th International Conference on Offshore mechanics and Arctic Engineering, The Hague, March 1989, Vol. 5, pages 121-127.

Leech, C.M., Hearle, J.W.S., Overington, M.S. and Banfield, S.J. (1993). "Modelling Tension and Torque Properties of Fibre Ropes and Splices", Proc. Third Int. ISOPE Conf., 370 - 376.

Riewald, P.G. (1986). "Performance Analysis of an Aramid Mooring Line", 18th Annual OTC, Houston, Texas, May 1986, paper OTC 5187.

Riewald, P.G., Walden, R.G., Whitehill, A.S., and Koralek, A.S. (1986). "Design and Deployment Parameters Affecting the Survivability of Stranded Aramid Fibre Ropes in the Marine Environment", IEEE OCEANS '86 Conference Proceedings, Washington D.C., September 1986, page 284.

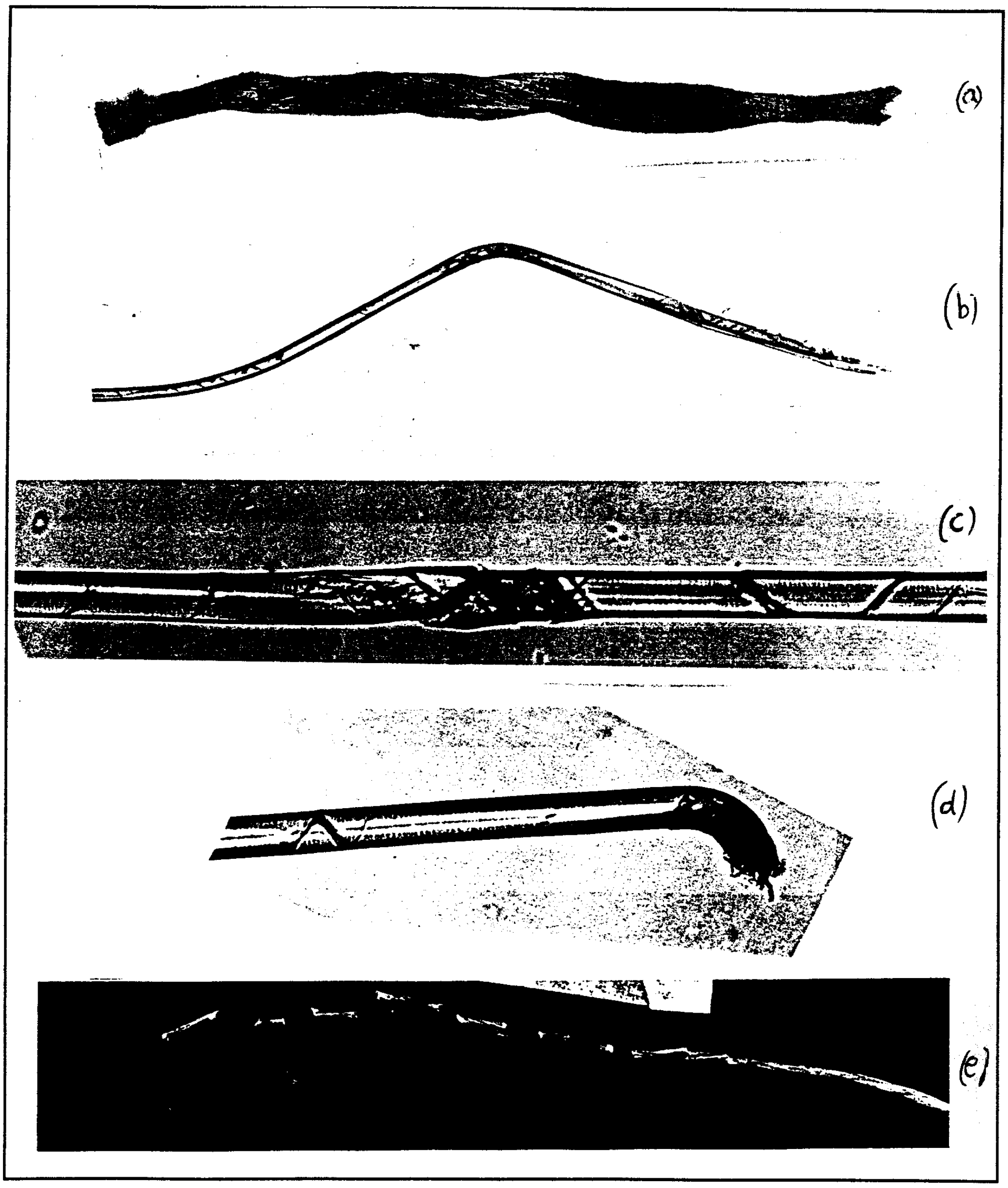


**Figure 1** Axial compression fatigue effects in 7-strand aramid ropes after tension-tension cycling: (a) Dyed bands, indicating fibre damage, at intervals along yarns; (b) Straight section leading to a kink along a fibre; (c) Internal kink-bands in uniform axial compression; (d) Fibre rupture at a sharp kink; (e) Yarn broken into multiple short pieces, followed by unbroken section. From Hearle and Noone (to be published).

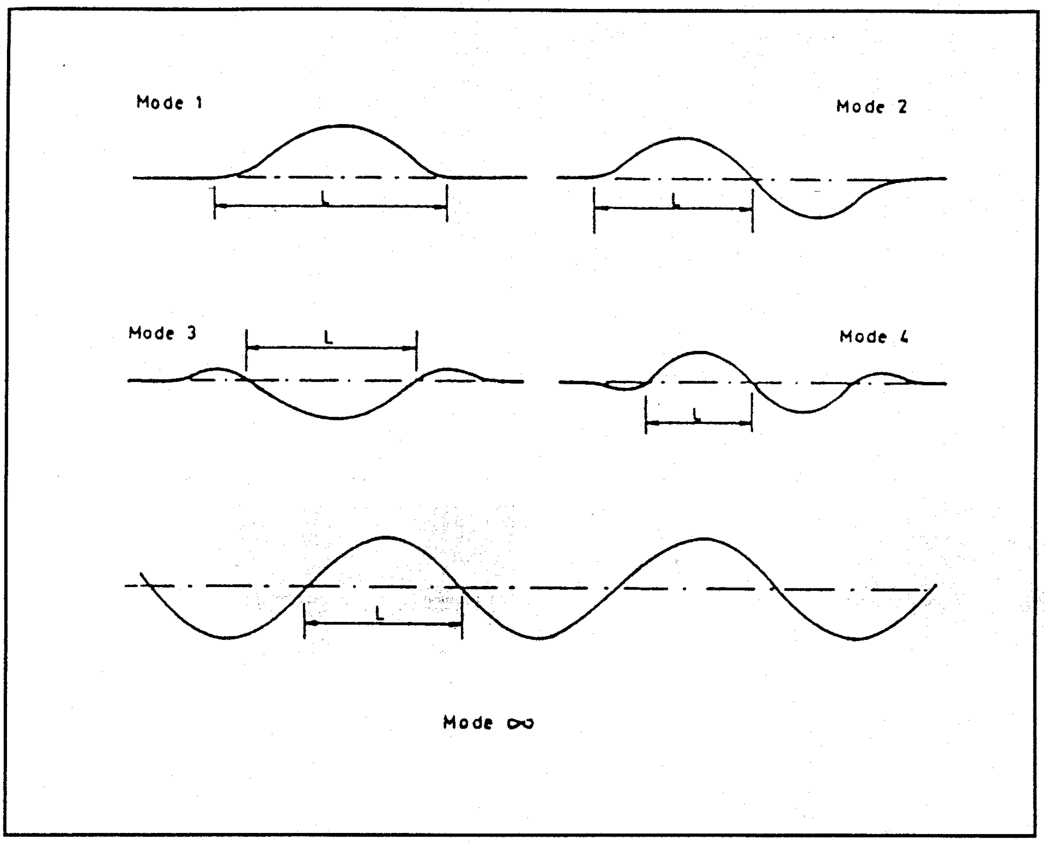


**Figure 2** Elastic buckling modes, from Hobbs (1984)

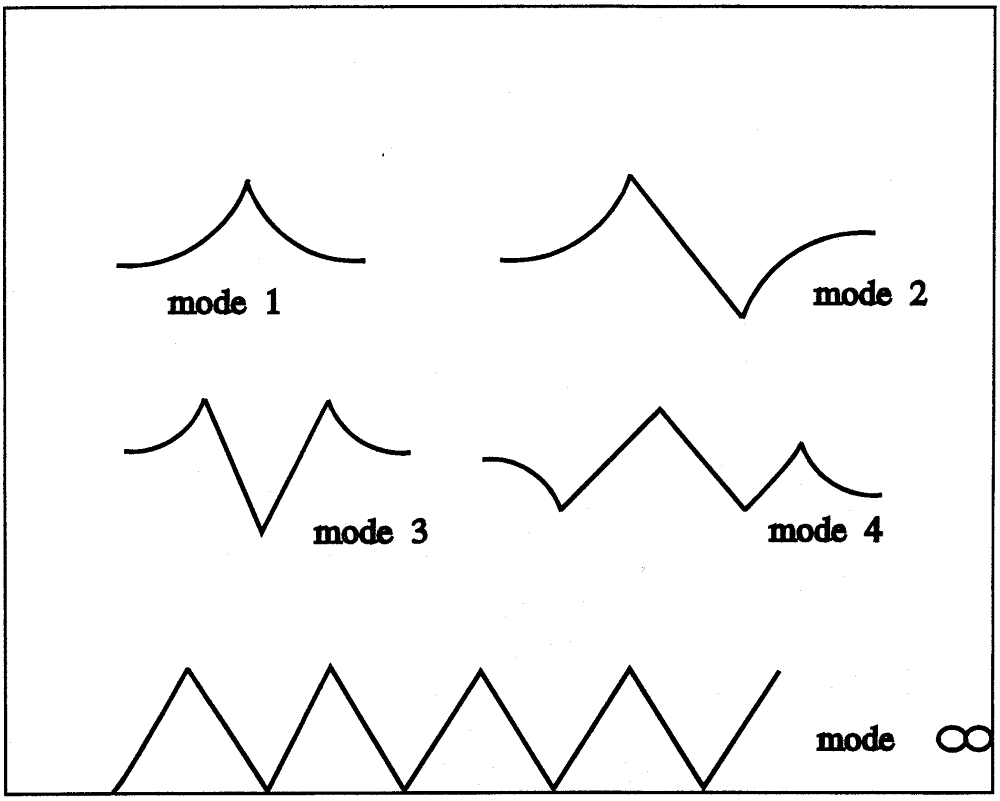


**Figure 3** Plastic buckling modes with kinks

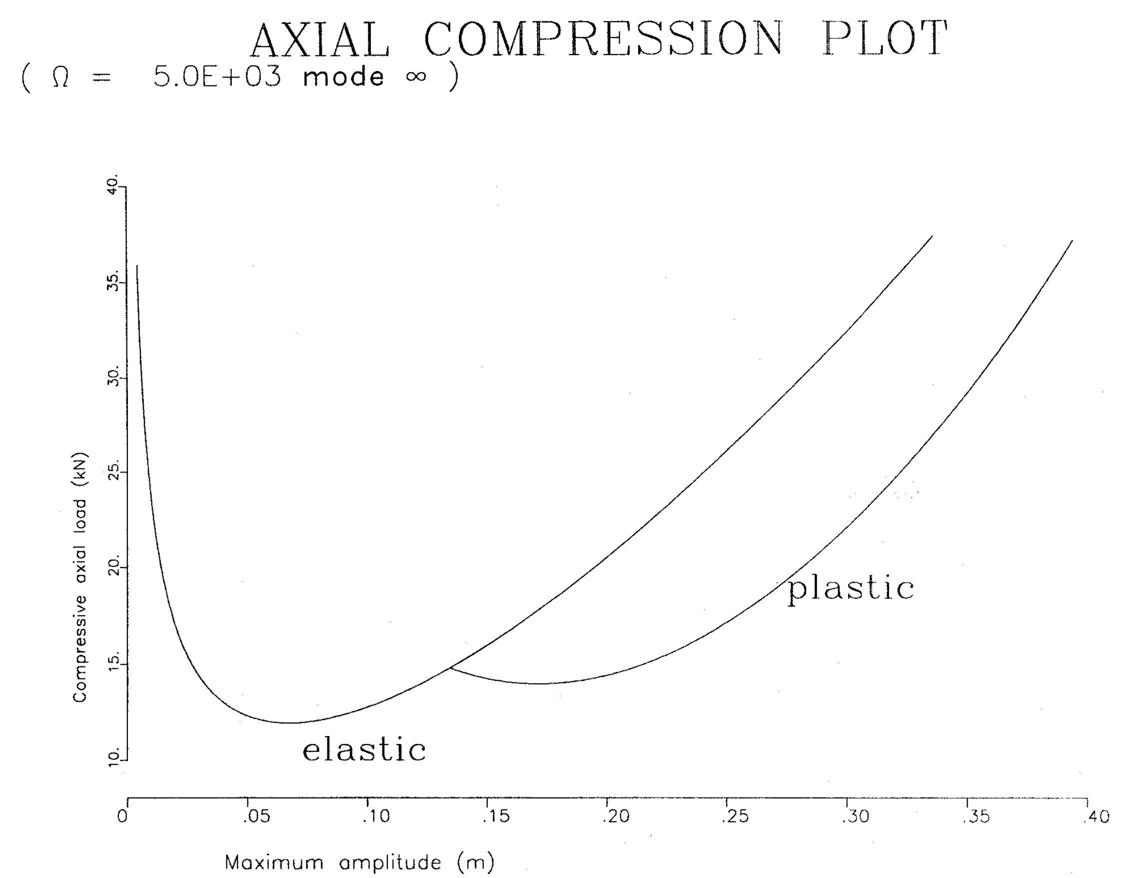


**Figure 4** Example of compressive axial load v. maximum amplitude.

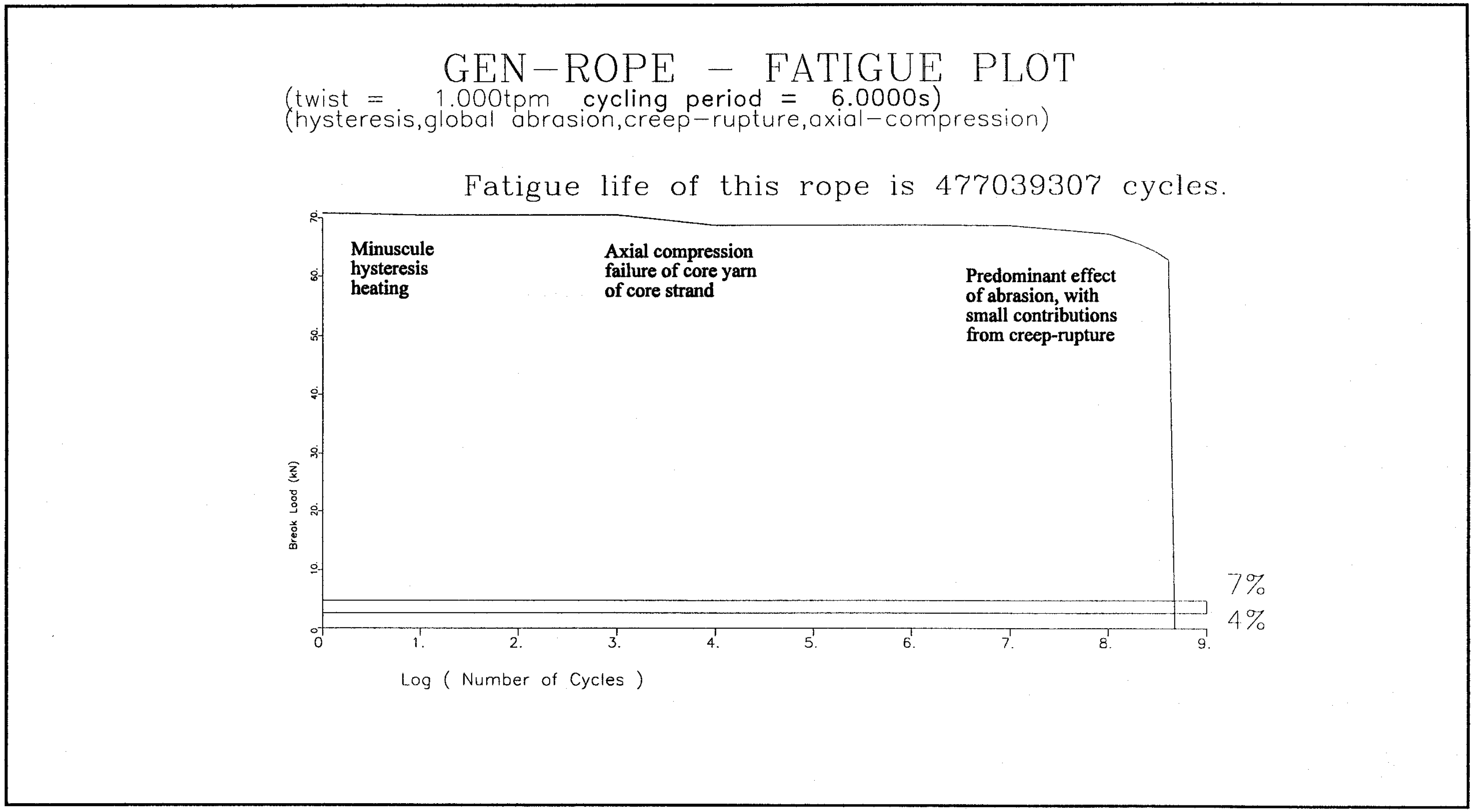


**Figure 5** Life prediction for 7-strand aramid rope showing effects of hysteresis heating, axial compression fatigue, abrasion and creep rupture.

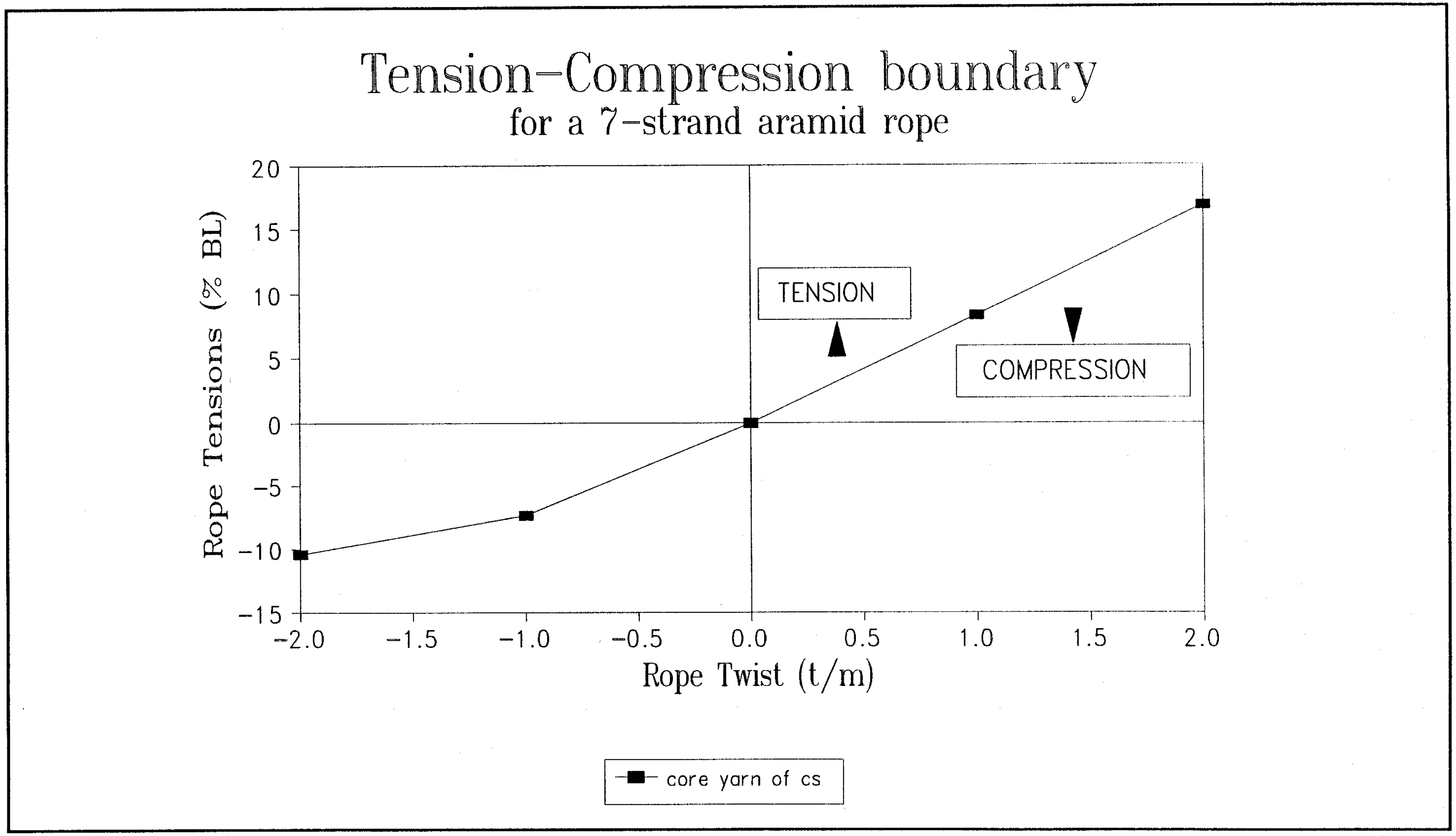


**Figure 6**(a) Tension-compression boundary for a 7-strand aramid rope, as a function of tension and twist.

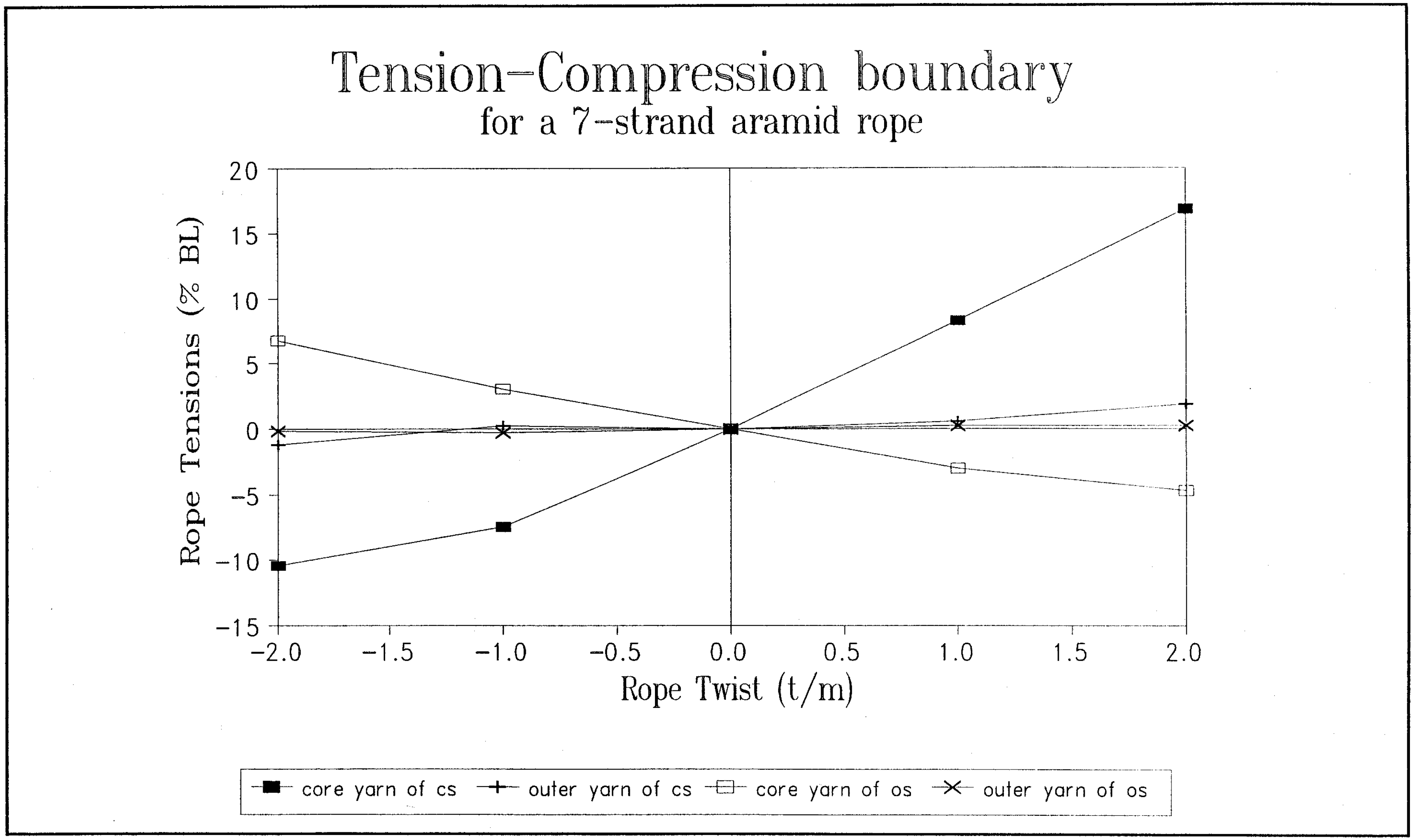


**Figure 6**(b) Tension-compression boundaries for four types of rope component.

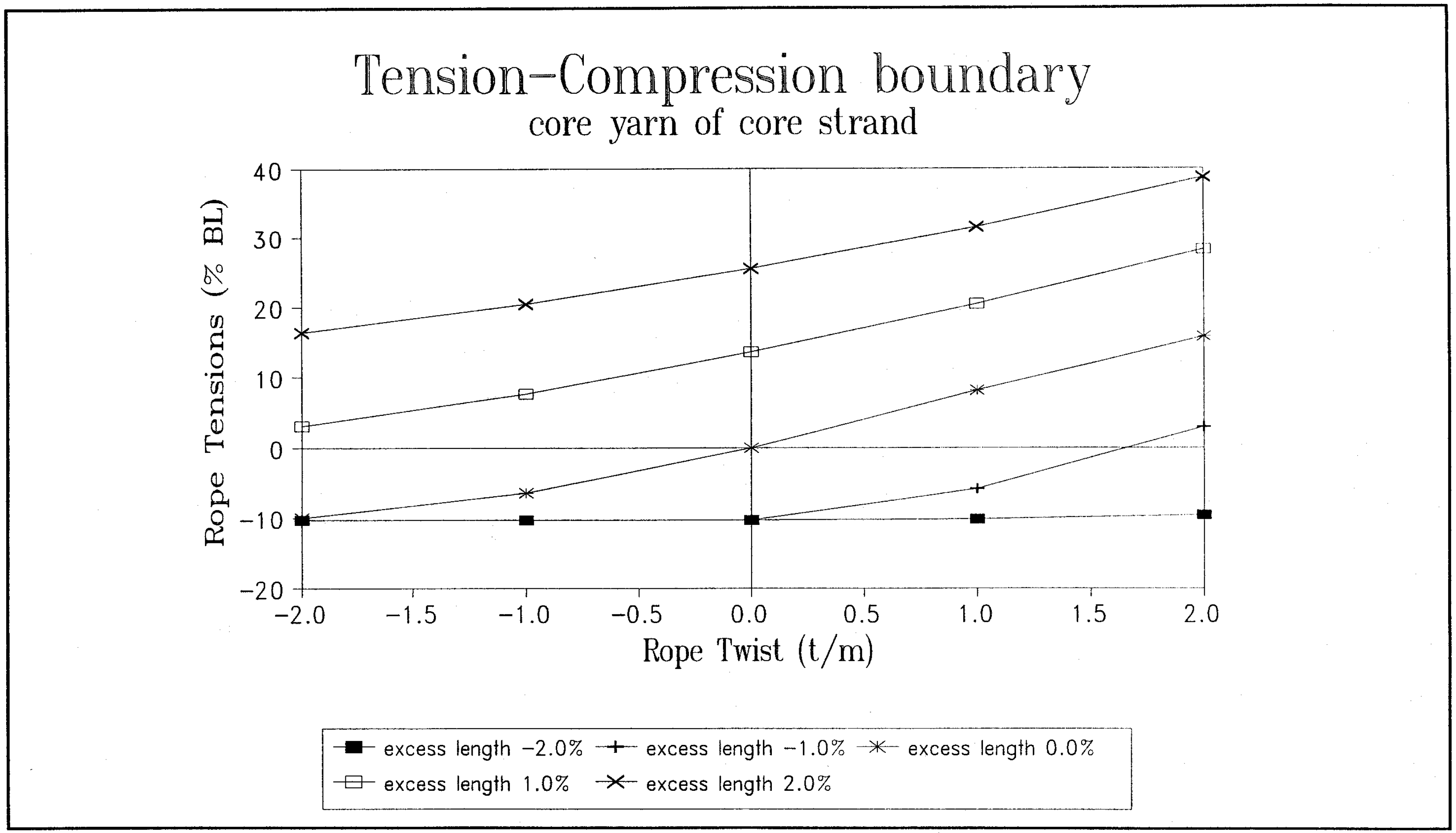


**Figure 6**(c) Tension-compression boundaries with various levels of excess length in the core yarn of the core strand of a 7-strand polyester rope.